

ORIGINAL ARTICLE

Zbtb16 has a role in brown adipocyte bioenergetics

CL Plaisier^{1,6}, BJ Bennett^{1,7}, A He², B Guan², AJ Lusis^{1,3,4,5}, K Reue^{1,3,5} and L Vergnes¹

OBJECTIVE: A better understanding of the processes influencing energy expenditure could provide new therapeutic strategies for reducing obesity. As the metabolic activity of the brown adipose tissue (BAT) and skeletal muscle is an important determinant of overall energy expenditure and adiposity, we investigated the role of genes that could influence cellular bioenergetics in these two tissues.

DESIGN: We screened for genes that are induced in both the BAT and skeletal muscle during acute adaptive thermogenesis in the mouse by microarray. We used C57BL/6J mice as well as the primary and immortalized brown adipocytes and C2C12 myocytes to validate the microarray data. Further characterization included gene expression, mitochondrial density, cellular respiration and substrate utilization. We also used a Hybrid Mouse Diversity Panel to assess *in vivo* effects on obesity and body fat content.

RESULTS: We identified the transcription factor *Zbtb16* (also known as *Plzf* and *Zfp14*) as being induced in both the BAT and skeletal muscle during acute adaptive thermogenesis. *Zbtb16* overexpression in brown adipocytes led to the induction of components of the thermogenic program, including genes involved in fatty acid oxidation, glycolysis and mitochondrial function. Enhanced *Zbtb16* expression also increased mitochondrial number, as well as the respiratory capacity and uncoupling. These effects were accompanied by decreased triglyceride content and increased carbohydrate utilization in brown adipocytes. Natural variation in *Zbtb16* mRNA levels in multiple tissues across a panel of >100 mouse strains was inversely correlated with body weight and body fat content.

CONCLUSION: Our results implicate *Zbtb16* as a novel determinant of substrate utilization in brown adipocytes and of adiposity *in vivo*.

Nutrition and Diabetes (2012) 2, e46; doi:10.1038/nutd.2012.21; published online 17 September 2012

Keywords: *Zbtb16*; *Plzf*; brown adipose tissue; adaptive thermogenesis; bioenergetics

INTRODUCTION

The increasing prevalence of obesity worldwide reflects changes in lifestyle, including a combination of increased food intake and reduced physical activity.^{1–3} This combination contributes to the accumulation of an energy surplus in the form of adipose tissue. Because obesity develops when energy intake exceeds energy expenditure, increasing energy expenditure is an attractive strategy to reduce body weight and fat storage. There has been considerable interest in modulating thermogenesis, particularly in the skeletal muscle and brown adipose tissue (BAT), as a target for the treatment of obesity.^{4–6}

Skeletal muscle is one of the central tissues involved in shivering thermogenesis and also contributes to non-shivering thermogenesis.^{5,7,8} Skeletal muscle is responsible for at least 30% of the basal metabolic energy expenditure and 80% of whole-body glucose uptake.⁹ Because skeletal muscle accounts for approximately 30–40% of total body mass, it may contribute substantially to adaptive thermogenesis in humans.⁵ Recently, the existence of BAT in humans has been reappraised and there is good evidence that brown fat depots are active in adults and are capable of energy dissipation through adaptive thermogenesis.^{10–13} Furthermore, body-mass index and percentage of body fat are inversely correlated with the BAT in humans¹², suggesting that the

BAT contributes to metabolic rate and is an important regulator of body fat accumulation. Further evidence for a shared physiological function between brown adipocytes and myocytes is the fact that they are derived from a common cell lineage.^{14,15} Increased heat production through decreased coupling between fatty acid oxidation and ATP synthesis has been observed during both diet-induced and cold-induced adaptive thermogenesis.^{16,17} During adaptive thermogenesis, a significant amount of energy stored as fat and glycogen is converted to heat instead of being efficiently converted to ATP, suggesting that induction of mitochondrial respiration or the level of uncoupling activity could promote caloric dissipation.

Because of its potential for energy dissipation, it is of great interest to identify the genes that orchestrate the changes occurring during adaptive thermogenesis and to determine their mechanisms of action. One key factor in adaptive thermogenesis of the BAT is the mitochondrial *uncoupling protein-1* (*Ucp1*). *Ucp1* is responsible for enabling the proton leak in mitochondria that dissipates energy produced through oxidative metabolism to generate heat.^{17–19} Previous systematic studies have identified genes that are induced in BAT after cold exposure in mouse, rat and squirrel,^{20–26} and a recent transcriptome-profiling study identified several genes that are induced in the skeletal muscle and BAT in mice.²⁷

¹Department of Human Genetics, David Geffen School of Medicine, University of California, Los Angeles, CA, USA; ²Department of Applied Genomics, Bristol Myers-Squibb, Pennington, NJ, USA; ³Department of Medicine, University of California, Los Angeles, CA, USA; ⁴Department of Microbiology, Immunology and Molecular Genetics, David Geffen School of Medicine, University of California, Los Angeles, CA, USA and ⁵Department of Molecular Biology Institute, University of California, Los Angeles, CA, USA. Correspondence: Dr L Vergnes, Department of Human Genetics, David Geffen School of Medicine, University of California, Los Angeles, CA 90095, USA. E-mail: lvergnes@ucla.edu

⁶Current address: Institute for Systems Biology, Seattle, WA 98109, USA

⁷Current address: Department of Genetics, University of North Carolina, Chapel Hill, NC 28081, USA

Received 16 August 2012; accepted 18 August 2012

We hypothesized that understanding the function of genes promoting energy expenditure would reveal new targets for modulation of energy balance. Genes differentially expressed in both the BAT and skeletal muscle could be of great importance because they are indicative of a general thermogenic response not limited to the BAT-specific uncoupling or skeletal muscle-specific shivering. We performed transcriptional profiling of the BAT and skeletal muscle during acute cold exposure in mice, a model of adaptive thermogenesis. We identified genes that were induced in both the BAT and skeletal muscle following cold exposure. One of the significantly upregulated genes is the transcription factor *Zbtb16*, which belongs to the POZ/domain and Krüpel zinc finger family and generally acts as a repressor.^{28–30} Here, we demonstrate that *Zbtb16* levels influence cellular bioenergetics *in vitro* and inversely correlate with adiposity *in vivo*.

MATERIALS AND METHODS

Mice

Animal studies were performed under approved UCLA animal research protocols and according to guidelines established in the Guide for Care and Use of Laboratory Animals. C57BL/6J mice were maintained in 12-h light/dark conditions and fed a regular chow diet (Purina 50010, Lab Diet, Richmond, IN, USA). Cold exposure was performed as described.³¹ After euthanasia, tissues were collected and frozen until use.

Microarray analysis

Total RNA was isolated from mouse tissues by extraction with TRIzol (Invitrogen, Carlsbad, CA, USA). Samples were then hybridized to Illumina 24K BeadChips using standard protocols (The Southern California Genotyping Consortium at UCLA). Differentially expressed genes were identified by applying a Student's *t*-test and fold-change thresholds. The microarray data can be accessed from the NCBI Gene Expression Omnibus (GEO) database.

Cell culture and over-expression

Primary brown adipocytes were cultured as described previously.³¹ C2C12 cells (ATCC, Manassas, VA, USA) were grown in complete DMEM (Dulbecco's modified Eagle's medium; 10% fetal bovine serum, 25 mM glucose, 1 mM pyruvate and 1 mM glutamine). For differentiation, serum was switched to 2% horse serum for 6 days. The immortalized brown adipocyte cell line was a gift from Bruce Spiegelman and was cultured as described.³²

Mouse *Zbtb16* cDNA was cloned into pcDNA3.1/V5-His vector (Invitrogen) and transfected with BioT (Bioland, La Palma, CA, USA). Empty vector was used as control. For transduction, an adenovirus was constructed from the *Zbtb16* cDNA and the AdEasy XL Adenoviral Vector System (Stratagene, Santa Clara, CA, USA). Viral particles were purified with Adeno-X Maxi Purification Kit (Clontech, Mountain View, CA, USA) and titered with Adeno-X Rapid Titer Kit (Clontech). Transduction (MOI 50) was performed at day 3 post-confluence and gene expression analyzed at day 6.

Quantitative real-time (qRT-PCR) gene expression analyses

Total RNA was isolated from mouse tissues by extraction with TRIzol (Invitrogen). For human tissues, a cDNA panel was purchased from Clontech. cDNA synthesis, real-time PCR, and qRT-PCR were performed as described previously.³³ Values are expressed in arbitrary units, normalized to housekeeping genes. All primer sequences used in this study are presented in Supplementary Table S1.

Immunoblotting

Cells were lysed in lysis buffer containing protease inhibitor cocktail (Roche, Indianapolis, IN, USA). Proteins (50 µg/lane) were resolved by 7% Tris-Acetate pre-cast gel (Invitrogen), transferred to nitrocellulose membrane and incubated for 3 h with 5% milk TBS-T (Tris-buffered saline with Tween 20), overnight with primary antibody in 1% milk TBS-T, then 1 h with a horseradish peroxidase-conjugated secondary antibody in 1% milk TBS-T. ECL Plus (GE Healthcare, Piscataway, NJ, USA) was used for chemiluminescent detection. Antibodies included ZBTB16 (OP128,

Calbiochem, Billerica, MA, USA), UCP1 (662045, Calbiochem), β-ACTIN (AC-15, Sigma, Dallas, TX, USA) and LAMIN A/C (sc-6215, Santa Cruz Biotechnology, Santa Cruz, CA, USA).

Triglyceride (TAG) contents and lipolysis assay

Cells were homogenized by sonification and TAG contents determined with L-Type triglyceride M kit (Waco Chemicals, Richmond, VA, USA). Lipolysis experiments from cell medium were performed after 10 h incubation with the Adipolysis Assay Kit (AB100, Millipore, Billerica, MA, USA). TAG contents and glycerol concentrations were normalized to protein.

Cellular oxygen consumption and extracellular acidification rates

Cellular metabolic rates were measured using a XF24 Analyzer (Seahorse Bioscience, Billerica, MA, USA). Immediately before the measurement, cells were washed with unbuffered DMEM as described.³⁴ Plates were placed into the XF24 instrument for measurement of oxygen consumption and extracellular acidification (ECAR) rates. Mixing, waiting and measurement times were 3, 2, and 3 min for C2C12 and 5, 2 and 1.5 min for brown adipocyte cells, respectively. The measures were normalized per protein. Test compounds were obtained from Sigma and injected during the assay at the following final concentration: 0.75 or 0.5 µM oligomycin, 0.5 or 0.4 µM FCCP (carbonyl cyanide 4-(trifluoromethoxy)phenylhydrazone), 0.75 or 0.15 µM rotenone/myxothiazol (differentiated brown adipocyte cells or C2C12, respectively), 25 mM glucose, 100 µM 2,4-dinitrophenol, 50 mM Na-oxamate, and 200 mM 2-deoxyglucose. The basal and percentage of oxygen consumption rate and ECAR levels as well as area under the curve were obtained with the XF24 Analyzer software.

Mitochondrial DNA content

Total genomic DNA from the BAT tissue was isolated by phenol/chloroform/isoamyl alcohol extraction. Mitochondrial and nuclear DNA were amplified by RT-PCR with 25 ng of DNA and primers in the D-Loop region and Tert gene, respectively (sequences in Supplementary Table S1).

Substrate utilization with Biolog microplates

PM-M TOX1 microplates (Biolog, Hayward, CA, USA), consisting of eight different substrates in replicate, were used. Differentiated brown adipocyte cells were seeded at 60 000 cells per well in complete medium without pyruvate, glucose or phenol red. After 24 h, Biolog Redox Dye MA was added and rates measured every hour at 590 nm to detect the metabolic activity. Time 0 was subtracted for each time point. The reductase activity (NADH) is proportional to the energy produced from each substrate.

Hybrid Mouse Diversity Panel

Mouse strains, RNA isolation and expression profiling were described previously.³⁵ Briefly, at 16 weeks of age, 4–6 mice per strain were assessed for body composition using an EchoMRI instrument (EchoMRI, Houston, TX, USA). Mice were fasted overnight before plasma and tissue collection. Tissues were weighed and then snap frozen in liquid nitrogen until RNA, cRNA and cDNA were prepared. Biotin-labeled cRNA was generated from the cDNA and used to probe by using Affymetrix Mouse Genome HT_MG430A arrays (4–6 mice per strain). Expression data (probe 1442025_a_at) and phenotypic traits are presented in Supplementary Table S2.

Statistical analysis

The data are expressed as the mean ± s.d., except for the XF24 Seahorse Bioscience analysis where s.e. was used. Unpaired Student's *t*-test was used to compare the difference between the groups.

RESULTS

Identifying genes differentially regulated in adaptive thermogenesis

We assayed the transcriptomes of mice exposed to cold using gene expression microarrays to identify genes differentially expressed during thermogenesis. In the BAT, 124 genes were upregulated and 176 were downregulated at least twofold in response to cold exposure. In the skeletal muscle (quadriceps), 69 genes were upregulated and 67 were downregulated at least

Table 1. Common differential expression in BAT and muscle tissue (P -value < 0.05 and change $> twofold$)

Entrez ID	Gene	Brown adipose tissue		Muscle tissue	
		Fold change	P-value	Fold change	P-value
235320	<i>Zbtb16</i>	5.6	1.7×10^{-2}	4.8	2.3×10^{-2}
24082	<i>Gtlf3a</i>	3.7	3.6×10^{-2}	6.6	4.5×10^{-2}
20305	<i>Ccl6</i>	2.3	3.3×10^{-3}	4.5	2.8×10^{-3}
227731	<i>Slc25a25</i>	2.1	4.4×10^{-2}	13.9	4.2×10^{-2}
17750	<i>Mt2</i>	2.1	2.2×10^{-2}	2.5	2.0×10^{-2}
20846	<i>Stat1</i>	-2.5	3.0×10^{-2}	-2.6	4.6×10^{-2}
51789	<i>Tnk2</i>	-2.6	2.5×10^{-2}	-2.1	2.5×10^{-2}
11481	<i>Acvr2b</i>	-2.7	4.2×10^{-2}	-2.9	2.3×10^{-2}
22341	<i>Vegf</i>	-3.6	1.9×10^{-2}	-2.9	1.5×10^{-2}
22418	<i>Wnt5a</i>	-3.6	1.2×10^{-3}	-2.3	4.0×10^{-2}
217198	<i>Plekhh3</i>	-4.8	1.1×10^{-2}	-2.2	1.9×10^{-3}

Abbreviation: BAT, brown adipose tissue.

twofold in response to cold exposure. We detected 11 genes that were altered by cold exposure in both the BAT and skeletal muscle, 5 of which were coordinately upregulated and 6 down-regulated (Table 1). The transcription factor *Zbtb16* (also known as *Plzf* and *Zfp145*) exhibited a robust induction in both the BAT (5.6-fold) and skeletal muscle (4.8-fold). *Zbtb16* has been associated with white adipogenesis³⁶ but has not previously been implicated in the BAT or muscle metabolism. We selected this gene to further characterize its function.

Validation of *Zbtb16* induction in adaptive thermogenesis

We first confirmed that *Zbtb16* expression is consistently upregulated by cold exposure at the mRNA and protein levels in an independent group of mice. As shown in Figure 1a, *Zbtb16* mRNA levels were increased 15.3-fold in the BAT and 2.1-fold in the muscle as detected by qPCR. *Zbtb16* mRNA induction by cold was observed after 4 or 8 h and whether mice were fasted or not during the cold exposure (data not shown). Western blot analysis confirmed a concomitant increase in ZBTB16 protein levels (Figure 1a, bottom inserts). Thus, the upregulation of *Zbtb16*

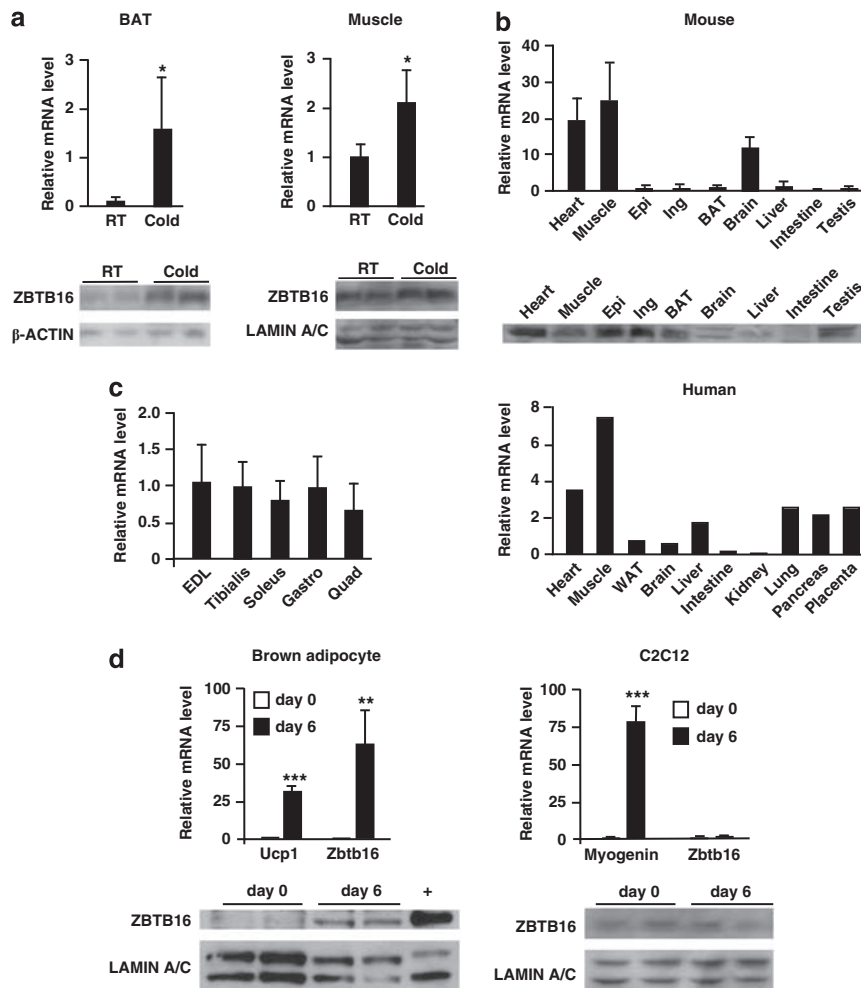


Figure 1. *Zbtb16* expression in tissues and cell lines. (a) Validation of *Zbtb16* mRNA upregulation in BAT and skeletal muscle by qRT-PCR (mean \pm s.d.; $n = 4$) and by immunoblot. (b) *Zbtb16* mRNA and protein levels in mouse (mean \pm s.d.; $n = 3$) and *Zbtb16* mRNA in human ($n = 1$) tissues. (c) *Zbtb16* mRNA levels in different skeletal muscles (mean \pm s.d.; $n = 4$). (d) *Zbtb16* mRNA levels and protein levels during brown adipocyte and C2C12 differentiation (mean \pm s.d., $n = 4$). Ucp1 and myogenin mRNA levels are differentiation controls for brown adipocyte and C2C12 cells, respectively. * $P < 0.05$; ** $P < 0.01$; *** $P < 0.001$ compared with control. EDL, extensor digitorum longus; Epi, epididymal fat; Gastro, gastrocnemius; Ing, inguinal fat; Quad, quadriceps; Tibialis, tibialis anterior; WAT, white adipose tissue.

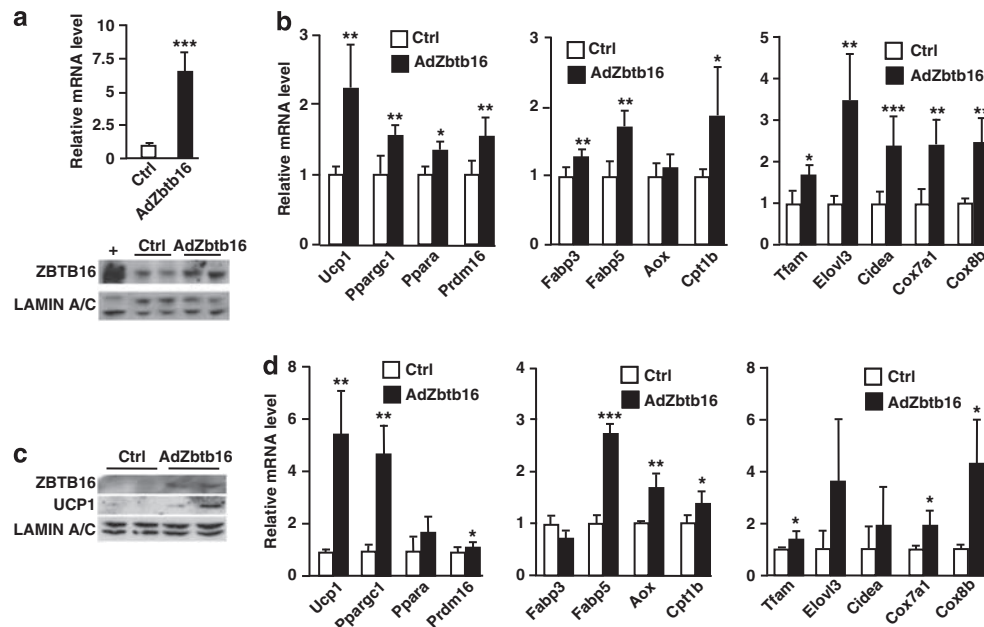


Figure 2. *Zbtb16* expression increases the gene program of brown adipocyte cells. **(a)** *Zbtb16* mRNA and protein levels after adenovirus transduction in differentiated immortalized brown adipocytes. **(b)** mRNA levels of brown adipocyte, fatty acid oxidation and mitochondrial markers in immortalized brown adipocytes (mean \pm s.d., $n=4$). **(c)** ZBTB16 and UCP1 protein levels after adenovirus transduction in differentiated primary brown adipocytes. **(d)** mRNA levels of brown adipocyte, fatty acid oxidation and mitochondrial markers in differentiated primary brown adipocytes (mean \pm s.d., $n=4$). * $P<0.05$; ** $P<0.01$; *** $P<0.001$ compared with control.

during adaptive thermogenesis was validated at both the transcript and protein levels.

Tissue expression pattern of *Zbtb16* in mouse and human

We then investigated whether the BAT and skeletal muscle were the most biologically relevant tissues for studying *Zbtb16* function by comparing mRNA expression levels in mouse and human tissue panels by qPCR. The highest *Zbtb16* expression levels were detected in the skeletal muscle and heart for both mouse and human (Figure 1b). In contrast to what Mikkelsen, *et al.*³⁶ reported, we detected a lower expression level in the mouse BAT than in the skeletal muscle. However, the levels of ZBTB16 protein measured by immunoblot in the white adipose tissue and BAT were similar to those of the heart and skeletal muscle (Figure 1b, insert). Within the muscle, the expression of *Zbtb16* was similar in fast twitch (extensor digitorum longus and tibialis), slow twitch (soleus) and mixed (quadriceps and gastronecnius) muscles (Figure 1c), suggesting that *Zbtb16* may function across muscle fiber types.

Expression of *Zbtb16* during brown adipocyte and myocyte differentiation

We then studied *Zbtb16* function *in vitro* using a mouse brown adipocyte cell line³² and the mouse C2C12 myocyte cell line. We first assessed *Zbtb16* expression dynamics during differentiation of brown adipocyte precursors into mature brown adipocytes. *Zbtb16* expression was dramatically upregulated 60-fold during brown adipocyte differentiation, whereas *Ucp1* showed a 30-fold induction (Figure 1d). By contrast, *Zbtb16* mRNA levels did not change during differentiation of C2C12 myoblasts to myotubes, whereas myogenin, used as control, was dramatically induced. The increased mRNA levels in brown adipocytes were mirrored by a substantial increase in ZBTB16 protein levels (Figure 1d, bottom inserts). The induction of *Zbtb16* during brown adipogenesis is consistent with a role for this protein in mature brown adipocytes.

Zbtb16 expression activates the brown adipocyte gene expression program

To begin to elucidate the effect of *Zbtb16* induction during thermogenesis, we overexpressed *Zbtb16* in brown adipocyte cells using an adenoviral vector carrying *Zbtb16* cDNA. We achieved roughly sixfold overexpression of *Zbtb16* mRNA (Figure 2a), which led to alterations in expression of genes involved in brown adipocyte differentiation and mitochondrial function. Indeed, compared with cells infected with a control lacZ-containing adenovirus, cells overexpressing *Zbtb16* exhibited significant upregulation of brown fat-enriched markers such as *Ucp1*, *Ppargc1a*, *Ppara* and *Prdm16* (*PR domain containing 16*; Figure 2b). Enhanced *Zbtb16* expression also stimulated the expression of genes promoting fatty acid oxidation, such as *Fabp3* (*fatty acid-binding protein 3*), *Fabp5* (also known as *Mal1*) and *Cpt1b* (*carnitine palmitoyltransferase 1b*). *Zbtb16* expression also elevated expression levels of mitochondrial gene markers such as *Tfam* (*mitochondrial transcription factor A*), *Elovl3* (*elongation of very long chain fatty acids-like 3*), *Cidea* (*cell death-inducing DFFA-like effector a*), *Cox7a1* (*cytochrome c oxidase, subunit VIIIa 1*) and *Cox8b* (*cytochrome c oxidase, subunit VIIIb*). To confirm these effects observed in an immortalized brown adipocyte cell line, we performed similar studies in primary brown adipocytes. *Zbtb16* adenoviral expression induced UCP1 protein levels (Figure 2c) and increased expression of brown fat, fatty acid oxidation and mitochondrial genes (Figure 2d). Thus, *Zbtb16* expression promotes a gene expression signature characteristic of active brown adipocytes and enhanced fatty acid oxidation.

Zbtb16 enhances mitochondrial respiration and mitochondrial biogenesis

The effect of *Zbtb16* on mitochondrial gene expression described above suggested that it may promote changes in brown adipocyte energetics. To assess this, we measured cellular respiration in brown adipocytes by real-time detection of oxygen consumption. Using a XF24 Seahorse Bioscience instrument, we

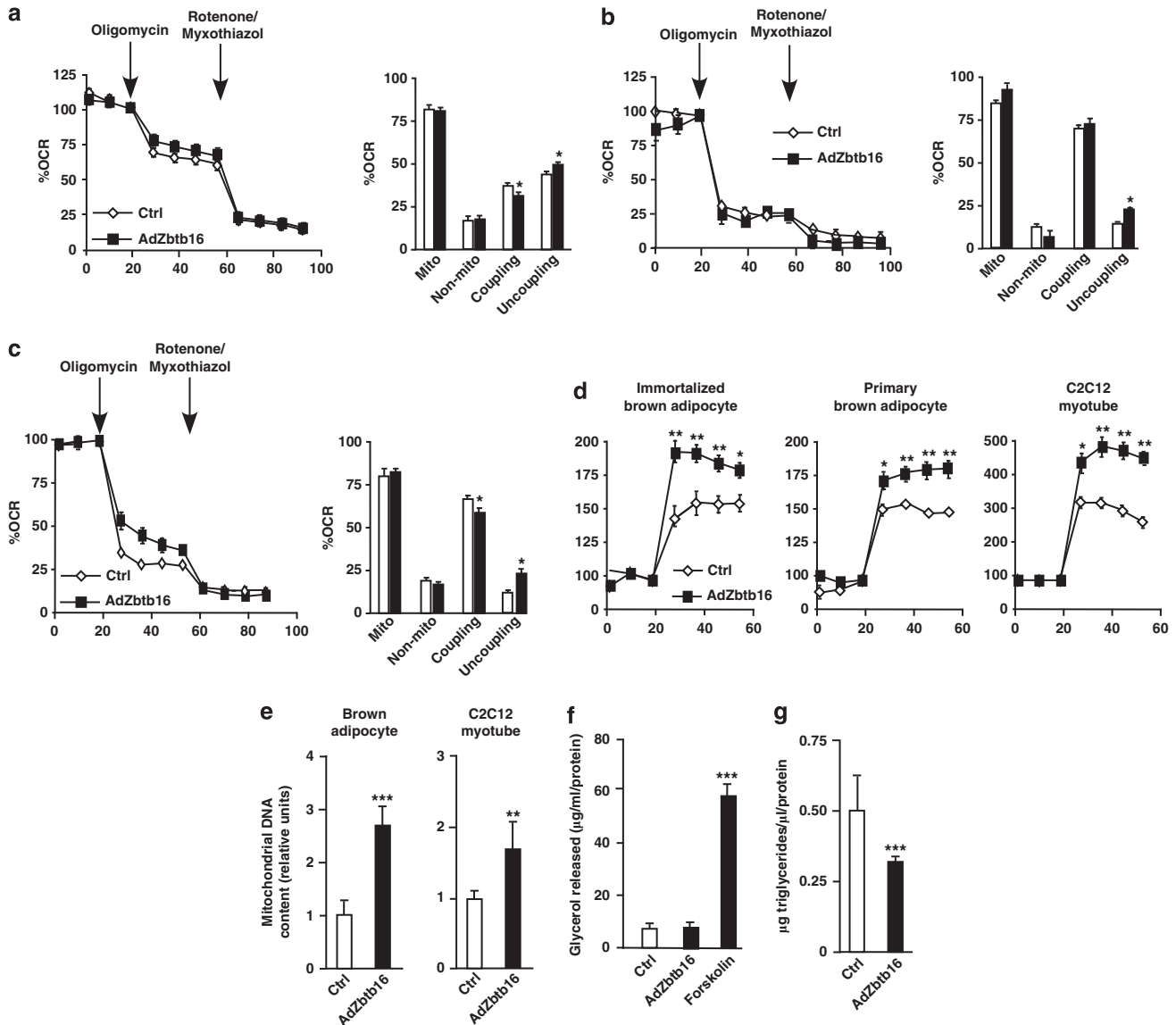


Figure 3. *Zbtb16* expression increases mitochondrial respiration. Oxygen consumption rate (OCR) values were recorded in cells transduced with control or *Zbtb16* adenovirus, before and after the sequential injection of oligomycin, and rotenone/myxothiazol, or FCCP alone. The measures are expressed as percentage of the baseline. **(a)** Brown adipocyte cells. **(b)** Primary brown adipocytes. **(c)** C2C12 myotubes. (mean \pm SE; $n=8$). **(d)** Percentage of change in OCR in immortalized and primary brown adipocytes, and C2C12 myotubes after injection of FCCP. **(e)** Relative mitochondrial DNA content measured by qRT-PCR. **(f)** Lipolysis assay after 10 h incubation. Forskolin treatment represents a positive control. **(g)** Triglyceride contents after 10 h of the lipolysis assay. * $P<0.05$; ** $P<0.01$; *** $P<0.001$ compared with control. Mito, mitochondrial respiration.

determined the level of different components of mitochondrial respiration contributing to the oxygen consumption using specific effectors. First, we determined the basal and coupling state of mitochondrial respiration with sequential injections of oligomycin and rotenone/myxothiazol. Oligomycin (F_1F_0 -ATP synthase inhibitor) allows the measurement of ATP-linked oxygen consumption (ATP turnover) and rotenone/myxothiazol (complex I and III inhibitor, respectively) by blocking mitochondrial respiration infers the non-mitochondrial respiration and the mitochondrial uncoupling (difference between oligomycin and rotenone/myxothiazol injections). Cells were 'activated' 2 h before the first measurement with 10 nM of the adrenoceptor agonist CL316,243. In both the immortalized and primary brown adipocytes, *Zbtb16* overexpression did not alter basal mitochondrial respiration, but showed higher mitochondrial uncoupling at the expense of coupling respiration (Figures 3a and b). C2C12 cells can also be 'activated' by beta-adrenergic stimulation when they are differentiated in

myotubes.³⁷ When we pretreated the myotubes for 1 h with 100 nM isoproterenol, we also observed a significant increase in mitochondrial uncoupling owing to *Zbtb16* expression (Figure 3c). We also assessed mitochondrial reserve capacity by injecting the electron transport uncoupler FCCP. Brown adipocytes (primary and immortalized) and C2C12 cells over-expressing *Zbtb16* exhibited a higher FCCP response, indicating more mitochondrial respiratory capacity (Figure 3d). Altogether, these results demonstrate that *Zbtb16* is able to promote proton leak during mitochondrial respiration and increase mitochondrial respiration capacity.

The enhanced expression of mitochondrial gene markers and mitochondrial respiration capacity suggested a potential effect of *Zbtb16* on mitochondrial biogenesis. To assess mitochondrial density, we measured the relative abundance of mitochondrial-encoded gene *D-loop* to the nuclear-encoded telomerase transcriptase (*Tert*) by qPCR. *Zbtb16* expression resulted in

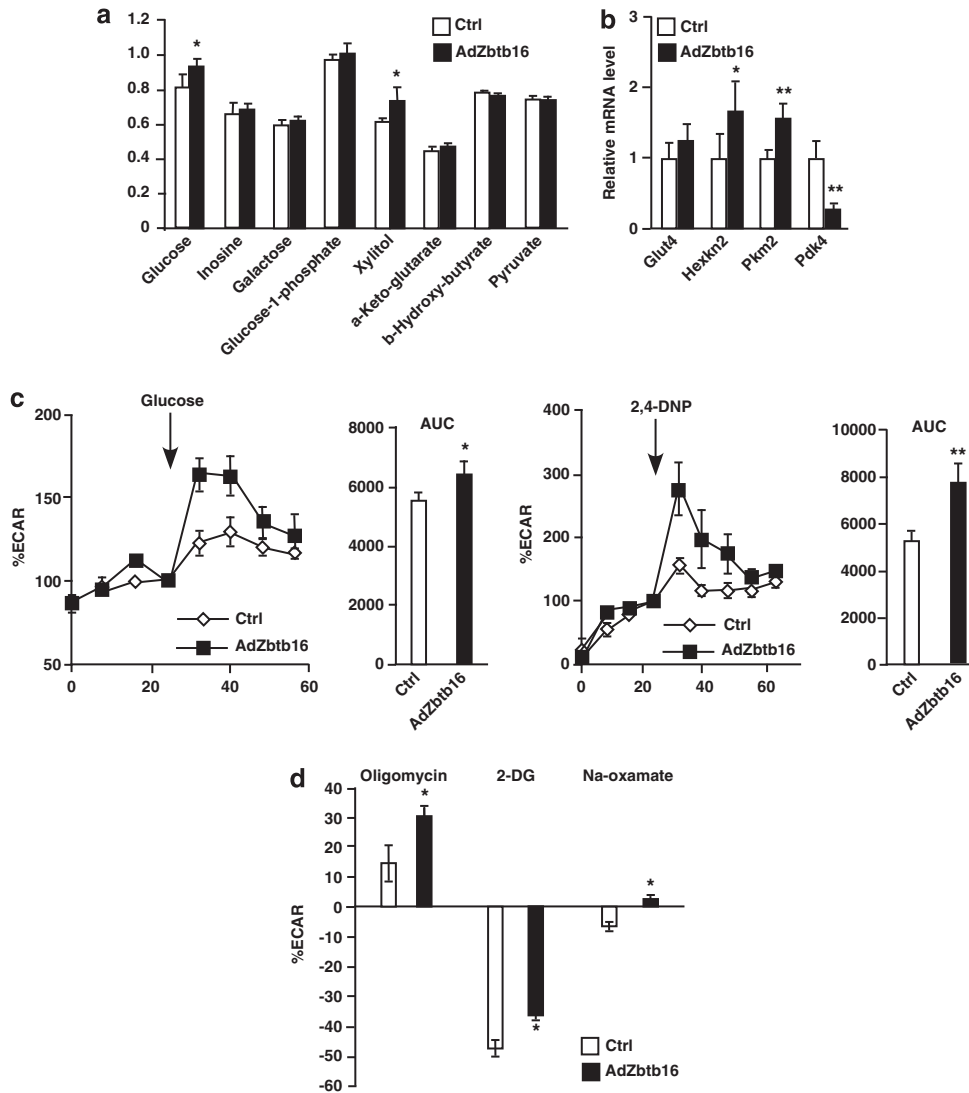


Figure 4. *Zbtb16* increases carbohydrate utilization. (a) Immortalized brown adipocyte cells transduced with control or *Zbtb16* adenovirus were dispensed in PM-M TOX1 plate and incubated for 1 day. Then, MA dye was added into the wells and the change in reductase activity due to energy (NADH) production after 10 h was recorded at 590 nm. (mean \pm s.d.; $n = 4$). (b) mRNA levels of glycolysis-related markers in immortalized brown adipocytes (mean \pm s.d.; $n = 4$). * $P < 0.05$; ** $P < 0.01$ compared with control. (c) ECAR values in immortalized brown adipocytes were recorded before and after glucose or 2,4-dinitrophenol (2,4-DNP) injection. (mean \pm SE; $n = 8$). The adjacent bar graphs represent the average area under the curve. (d) Percentage of change in ECAR values after injection of oligomycin, 2-deoxyglucose (2-DG) or Na-oxamate injection (mean \pm SE; $n = 6$). * $P < 0.05$; ** $P < 0.01$ compared with control.

increased mitochondrial DNA by threefold in brown adipocytes and by 1.7-fold in C2C12 myotubes (Figure 3e).

We next asked whether the increased mitochondrial respiration owing to *Zbtb16* overexpression affects lipolysis or lipid content in brown adipocytes. Lipolysis rates in brown adipocytes were not affected by *Zbtb16* expression, whereas forskolin elicited the expected increase (Figure 3f). However, intracellular TAG content was decreased by 40% in *Zbtb16* overexpressing cells (Figure 3g). Together, these data demonstrate that *Zbtb16* promotes biogenesis and respiration of mitochondria, and that higher expression of *Zbtb16* reduces cellular TAG levels in brown adipocytes.

Zbtb16 increases glucose oxidation

We then investigated whether *Zbtb16* affects substrate utilization. Control brown adipocytes or *Zbtb16* overexpressing cells were plated in Biolog microplates in which each well contains one of eight specific energy substrates. All the eight substrates were metabolized by brown adipocytes (Figure 4a and Supplementary

Figure S1). Overexpression of *Zbtb16* specifically increased utilization of glucose (glycolysis pathway) and xylitol (pentose phosphate pathway), while metabolism of other substrates was not affected by *Zbtb16*.

The preference in carbohydrate utilization suggests that *Zbtb16* may influence glucose metabolism. Therefore, we assayed the expression of genes controlling glycolysis in response to *Zbtb16* overexpression using qPCR. Levels of *Glut4* mRNA were not changed, but *Hexkin2* (*hexokinase II*) and *Pkm2* (*pyruvate kinase*) expression levels were increased by *Zbtb16* (Figure 4b). In addition, expression of *Pdk4* was decreased. Increased glucose utilization and the differential expression of glycolysis-specific enzymes support a role for *Zbtb16* in glucose consumption.

We then assessed the effects of *Zbtb16* overexpression on glucose metabolism by quantitating a measure of glycolysis, the ECAR. Addition of glucose or the mitochondrial uncoupler 2,4-dinitrophenol increased ECAR in differentiated brown adipocytes. This response was amplified in cells with increased *Zbtb16* expression, suggesting a greater ability to increase glycolysis

Table 2. Correlation between *Zbtb16* transcript levels and phenotypic traits

	Adipose		Heart	
	R	P-value	R	P-value
Body weight	-0.18	NS	-0.32	$1.3E \times 10^{-3}$
NMR-total fat fat	-0.20	NS	-0.33	8.2×10^{-4}
NMR-% body fat	-0.30	3.5×10^{-3}	-0.38	1.1×10^{-4}
Total fat mass	-0.22	3.5×10^{-2}	-0.38	8.5×10^{-5}
Gonadal fat pad	-0.27	7.8×10^{-3}	-0.36	2.3×10^{-4}
% Gonadal fat pad	-0.31	2.5×10^{-3}	-0.33	8.1×10^{-4}
Retroperineal fat pad	-0.25	1.3×10^{-2}	-0.35	4.7×10^{-4}
% Retroperineal fat pad	-0.23	2.5×10^{-2}	-0.39	7.4×10^{-5}
Femoral fat pad	-0.23	2.7×10^{-2}	-0.39	8.3×10^{-5}
% Femoral fat pad	-0.27	7.2×10^{-3}	-0.42	1.5×10^{-5}
Mesenteric fat pad	-0.26	NS	-0.42	1.2×10^{-5}
% Mesenteric fat pad	-0.09	NS	-0.41	2.2×10^{-5}

Abbreviations: NMR, nuclear magnetic resonance; NS, not significant. R, correlation coefficient; % corresponds to total body weight.

(Figure 4c). We therefore exposed the brown adipocytes to different modulators of glycolysis and measured the ECAR response. Cells overexpressing *Zbtb16* had a greater response to treatment with oligomycin which inhibits mitochondrial ATP production, suggesting an increased glycolytic capacity when ATP demand increases (Figure 4d). When treated with the glucose analog 2-deoxyglucose, which inhibits glycolysis, the effect was slightly less pronounced in cells expressing *Zbtb16* (Figure 4d). We also performed experiments with Na-oxamate, an inhibitor of lactate dehydrogenase, which catalyzes the conversion of pyruvate to lactic acid. Na-oxamate did not significantly inhibit ECAR in brown adipocytes (~7%), suggesting that the final step of glycolysis does not account for a substantial amount of glycolysis detected by the ECAR and that anaerobic glycolysis is not very active in these cells. Nevertheless, this modest inhibition was abrogated when *Zbtb16* was overexpressed (Figure 4d). Together, these results suggest that *Zbtb16* promotes glucose oxidation, consistent with the increased mitochondrial respiration and lower *Pdk4* expression.

Zbtb16 expression correlates with body weight, fat mass and diabetes *in vivo*

As described above, our data indicate that *Zbtb16* is involved in the adaptive thermogenesis response and promotes mitochondrial respiration and carbohydrate utilization in brown adipocytes. To assess the role of *Zbtb16* on energy balance *in vivo*, we assessed whether genetic variations in *Zbtb16* gene expression levels are correlated with clinical traits. For these studies, we examined *Zbtb16* expression levels in a Hybrid Mouse Diversity Panel.³⁵ This resource consists of more than 100 highly diverse inbred and recombinant inbred mouse strains, which allow the analysis of association between gene expression levels and metabolic traits such as plasma lipids, plasma hormones and different body fat parameters.^{35,38} We investigated the correlations between *Zbtb16* expression levels and obesity traits in two tissues available in this panel that are most relevant to our study: as the BAT and skeletal muscle were not available in the hybrid mouse diversity panel, we examined the white adipose tissue and heart. The most robust associations for *Zbtb16* were inverse correlations with body weight and fat mass (measured by nuclear magnetic resonance and weight) in both the tissues (Table 2 and Supplementary Figure S2). The inverse correlation for fat mass included gonadal, retroperitoneal, femoral and mesenteric fat pads. This finding demonstrates that common, natural variations in *Zbtb16* expression levels are correlated with body fat content in the mouse.

Given the association of *Zbtb16* mRNA levels with body weight and fat mass, we also assessed whether *ZBTB16* expression levels are associated with fat mass in humans as well. Data mining from previously reported microarray analyses revealed that in visceral adipose tissue of obese diabetic women, *ZBTB16* expression was significantly lower than age- and body-mass index-matched normal glucose-tolerant controls (*t*-test *P*-value = 0.0056; GEO accession GDS3665). This result demonstrates that in humans, *ZBTB16* expression levels are associated with glucose levels, suggesting a complex interrelationship between *ZBTB16* expression, glucose and obesity.

DISCUSSION

Manipulation of cellular bioenergetics is an attractive approach to increase cellular energy expenditure with the ultimate goal to decrease obesity at the whole body level. Mitochondrial respiration, primarily in the BAT and skeletal muscle, can be modified in order to respond to physical activity, diet or ambient temperature. In the current work, we identified *Zbtb16* as a novel gene involved in the cold response in both the BAT and skeletal muscle. *Zbtb16* was among a few genes that were transcriptionally induced by several-fold in both the BAT and skeletal muscle during acute cold exposure. Previous works on *Zbtb16* have shown potential involvement in cancer and development. The human *ZBTB16* gene has been implicated in acute promyelocytic leukemia, through chromosomal translocation and fusion to the retinoic receptor alpha.^{39,40} Mice lacking *Zbtb16* function exhibit limb defects and loss of spermatogonial stem cells.^{41,42} Interestingly, *Zbtb16* is induced during differentiation of 3T3-L1 preadipocytes.³⁶ The role of *Zbtb16* as a transcription factor provides a potential mechanism by which it may influence thermogenesis, through effects on expression of other genes. Indeed, we found that induction of *Zbtb16* expression in brown adipocytes enhances the expression of many genes of the thermogenic program, such as genes involved in fatty acid oxidation and mitochondrial respiration. This effect was accompanied by an increase in mitochondrial content and maximal respiration capacity, and a decrease in intracellular TAG levels, consistent with a role for *Zbtb16* in fatty acid metabolism in brown adipocytes. When differentiated brown adipocytes or myotubes were activated by adrenoceptor agonists, *Zbtb16* increased mitochondrial uncoupling, in agreement with the increased *Ucp1* gene expression.

Another aspect of the role of *Zbtb16* is its function in glucose metabolism. *Zbtb16* expression drives the expression of glycolysis-related genes (*Hexkn2*, *Pkm2*), and is able to increase glycolytic capacity. Consistent with this role, *Zbtb16* expression increases carbohydrate utilization *in vitro*. The glucose utilization seems to be directed to mitochondrial oxidation as observed by the decrease in *Pdk4* expression and lower Na-oxamate-sensitive ECAR levels. Altogether, these results indicate that *Zbtb16* promotes oxidative metabolism.

Ultimately, the goal is to identify genes that influence energy metabolism in BAT that translates to whole-body effects on energy balance and adiposity. To evaluate the potential effect of variations in *Zbtb16* expression levels *in vivo*, we assessed the relationship between *Zbtb16* expression levels and body mass and fat pad mass across a set of > 100 mouse strains for which gene expression and body fat traits have been determined.³⁵ In this panel, we observed a striking association between *Zbtb16* mRNA levels in two different tissues and body fat parameters. Higher levels of *Zbtb16* expression were associated with a decrease in body fat storage in four major white adipose tissue depots and overall body weight. We also detected a correlation between decreased *ZBTB16* expression levels in human visceral adipose tissue and diabetic state among obese women. These results are consistent with a role for *Zbtb16* in increasing mitochondrial

respiration and substrate utilization. Interestingly, a congenic rat strain harboring a mutation in *Zbtb16* affected total body weight and adiposity, but it was not possible to rule out other mutations in the congenic strain.⁴³ Although global loss of *Zbtb16* function in mice⁴¹ and humans^{44,45} causes skeletal defects, more subtle variation in *Zbtb16* expression levels observed among individuals may be a determinant of adiposity. In the future, cell-type-specific knockout or transgenic models could be useful in determining further the role of *Zbtb16* in adipose tissue function, energy balance and obesity.

CONFLICT OF INTEREST

The authors declare no conflict of interest.

ACKNOWLEDGEMENTS

We thank Dr Bruce Spiegelman for the kind gift of the mouse brown adipocyte cell line and Dr Andrea Hevener for providing cDNA for mouse skeletal muscle subtypes. This work was supported by the American Heart Association Grant 09BGA2080363 (to LV), National Institutes of Health P01 HL28481 (to KR), and the National Center for research Resources Grant S10RR026744 (to KR).

REFERENCES

- Wyatt S, Winters KP, Dubbert PM. Overweight and obesity: prevalence, consequences, and causes of a growing public health problem. *Am J Med Sci* 2006; **331**: 166–174.
- Flegal KM, Carroll MD, Ogden CL, Curtin LR. Prevalence and trends in obesity among US adults, 1999–2008. *JAMA* 2010; **303**: 235–241.
- Hamilton MT, Hamilton DG, Zderic TW. Role of low energy expenditure and sitting in obesity, metabolic syndrome, type 2 diabetes, and cardiovascular disease. *Diabetes* 2007; **56**: 2655–2667.
- Costford S, Gowing A, Harper ME. Mitochondrial uncoupling as a target in the treatment of obesity. *Curr Opin Clin Nutr Metab Care* 2007; **10**: 671–678.
- Wijers SL, Saris WH, van Marken Lichtenbelt WD. Recent advances in adaptive thermogenesis: potential implications for the treatment of obesity. *Obes Rev* 2009; **10**: 218–226.
- Tseng YH, Cypess AM, Kahn CR. Cellular bioenergetics as a target for obesity therapy. *Nat Rev Drug Discov* 2010; **9**: 465–482.
- Clarke IJ, Henry BA. Targeting energy expenditure in muscle as a means of combating obesity. *Clin Exp Pharmacol Physiol* 2010; **37**: 121–124.
- van den Berg SA, van Marken Lichtenbelt W, Willems van Dijk K, Schrauwen P. Skeletal muscle mitochondrial uncoupling, adaptive thermogenesis and energy expenditure. *Curr Opin Clin Nutr Metab Care* 2011; **14**: 243–249.
- de Lange P, Moreno M, Silvestri E, Lombardi A, Goglia F, Lanni A. Fuel economy in food-deprived skeletal muscle: signaling pathways and regulatory mechanisms. *FASEB J* 2007; **21**: 3431–3441.
- Nedergaard J, Bengtsson T, Cannon B. Unexpected evidence for active brown adipose tissue in adult humans. *Am J Physiol Endocrinol Metab* 2007; **293**: E444–E452.
- Saito M, Okamatsu-Ogura Y, Matsushita M, Watanabe K, Yoneshiro T, Nio-Kobayashi J et al. High incidence of metabolically active brown adipose tissue in healthy adult humans: effects of cold exposure and adiposity. *Diabetes* 2009; **58**: 1526–1531.
- van Marken Lichtenbelt WD, Vanhommerig JW, Smulders NM, Drossaerts JM, Kemerink GJ, Bouvy ND et al. Cold-activated brown adipose tissue in healthy men. *N Engl J Med* 2009; **360**: 1500–1508.
- Cypess AM, Lehman S, Williams G, Tal I, Rodman D, Goldfine AB et al. Identification and importance of brown adipose tissue in adult humans. *N Engl J Med* 2009; **360**: 1509–1517.
- Gesta S, Tseng YH, Kahn CR. Developmental origin of fat: tracking obesity to its source. *Cell* 2007; **131**: 242–256.
- Timmons JA, Wennmalm K, Larsson O, Walden TB, Lassmann T, Petrovic N et al. Myogenic gene expression signature establishes that brown and white adipocytes originate from distinct cell lineages. *Proc Natl Acad Sci U S A* 2007; **104**: 4401–4406.
- Cannon B, Nedergaard J. Metabolic consequences of the presence or absence of the thermogenic capacity of brown adipose tissue in mice (and probably in humans). *Int J Obes (Lond)* 2010; **34**(Suppl 1): S7–16.
- Cannon B, Nedergaard J. Brown adipose tissue: function and physiological significance. *Physiol Rev* 2004; **84**: 277–359.
- Nicholls DG. A history of UCP1. *Biochem Soc Trans* 2001; **29**: 751–755.
- Klaus S, Casteilla L, Bouillaud F, Ricquier D. The uncoupling protein UCP: a membraneous mitochondrial ion carrier exclusively expressed in brown adipose tissue. *Int J Biochem* 1991; **23**: 791–801.
- Puigserver P, Wu Z, Park CW, Graves R, Wright M, Spiegelman BM. A cold-inducible coactivator of nuclear receptors linked to adaptive thermogenesis. *Cell* 1998; **92**: 829–839.
- Daikoku T, Shinohara Y, Shima A, Yamazaki N, Terada H. Specific elevation of transcript levels of particular protein subtypes induced in brown adipose tissue by cold exposure. *Biochim Biophys Acta* 2000; **1457**: 263–272.
- Adams SH, Chui C, Schilbach SL, Yu XX, Goddard AD, Grimaldi JC et al. BFIT, a unique acyl-CoA thioesterase induced in thermogenic brown adipose tissue: cloning, organization of the human gene and assessment of a potential link to obesity. *Biochem J* 2001; **360**: 135–142.
- Yu XX, Lewin DA, Forrest W, Adams SH. Cold elicits the simultaneous induction of fatty acid synthesis and beta-oxidation in murine brown adipose tissue: prediction from differential gene expression and confirmation *in vivo*. *FASEB J* 2002; **16**: 155–168.
- Watanabe M, Yamamoto T, Kakuha R, Okada N, Kajimoto K, Yamazaki N et al. Synchronized changes in transcript levels of genes activating cold exposure-induced thermogenesis in brown adipose tissue of experimental animals. *Biochim Biophys Acta* 2008; **1777**: 104–112.
- Yan J, Burman A, Nichols C, Alila L, Showe LC, Showe MK et al. Detection of differential gene expression in brown adipose tissue of hibernating arctic ground squirrels with mouse microarrays. *Physiol Genomics* 2006; **25**: 346–353.
- Navet R, Mathy G, Douette P, Dobson RL, Leprince P, De Pauw E et al. Mitoproteome plasticity of rat brown adipocytes in response to cold acclimation. *J Proteome Res* 2007; **6**: 25–33.
- Anunciado-Koza RP, Zhang J, Ukropec J, Bajpeyi S, Koza RA, Rogers RC et al. Inactivation of the mitochondrial carrier SLC25A25 (ATP-Mg2 + /Pi transporter) reduces physical endurance and metabolic efficiency in mice. *J Biol Chem* 2011; **286**: 11659–11671.
- Filipponi D, Hobbs RM, Ottolenghi S, Rossi P, Jannini EA, Pandolfi PP et al. Repression of kit expression by Plzf in germ cells. *Mol Cell Biol* 2007; **27**: 6770–6781.
- Scheffé JH, Menk M, Reinemund J, Efferzt K, Hobbs RM, Pandolfi PP et al. A novel signal transduction cascade involving direct physical interaction of the renin/prorenin receptor with the transcription factor promyelocytic zinc finger protein. *Circ Res* 2006; **99**: 1355–1366.
- Li JY, English MA, Ball HJ, Yeyati PL, Waxman S, Licht JD. Sequence-specific DNA binding and transcriptional regulation by the promyelocytic leukemia zinc finger protein. *J Biol Chem* 1997; **272**: 22447–2255.
- Vergnes L, Chin R, Young SG, Reue K. Heart-type fatty acid-binding protein is essential for efficient brown adipose tissue fatty acid oxidation and cold tolerance. *J Biol Chem* 2011; **286**: 380–390.
- Uldry M, Yang W, St-Pierre J, Lin J, Seale P, Spiegelman BM. Complementary action of the PGC-1 coactivators in mitochondrial biogenesis and brown fat differentiation. *Cell Metab* 2006; **3**: 333–341.
- Phan J, Peterfy M, Reue K. Lipin expression preceding peroxisome proliferator-activated receptor-gamma is critical for adipogenesis *in vivo* and *in vitro*. *J Biol Chem* 2004; **279**: 29558–29564.
- Wu M, Neilson A, Swift AL, Moran R, Tamagnine J, Parslow D et al. Multiparameter metabolic analysis reveals a close link between attenuated mitochondrial bioenergetic function and enhanced glycolysis dependency in human tumor cells. *Am J Physiol Cell Physiol* 2007; **292**: C125–C136.
- Bennett BJ, Farber CR, Orozco L, Kang HM, Ghazalpour A, Siemers N et al. A high-resolution association mapping panel for the dissection of complex traits in mice. *Genome Res* 2010; **20**: 281–290.
- Mikkelsen TS, Xu Z, Zhang X, Wang L, Gimble JM, Lander ES et al. Comparative epigenomic analysis of murine and human adipogenesis. *Cell* 2010; **143**: 156–169.
- Pearen MA, Ryall JG, Maxwell MA, Ohkura N, Lynch GS, Muscat GE. The orphan nuclear receptor, NOR-1, is a target of beta-adrenergic signaling in skeletal muscle. *Endocrinology* 2006; **147**: 5217–5227.
- Schadt EE, Lamb J, Yang X, Zhu J, Edwards S, Ghathakurta D et al. An integrative genomics approach to infer causal associations between gene expression and disease. *Nat Genet* 2005; **37**: 710–717.
- McConnell MJ, Licht JD. The PLZF gene of t (11;17)-associated APL. *Curr Top Microbiol Immunol* 2007; **313**: 31–48.
- Costoya JA, Pandolfi PP. The role of promyelocytic leukemia zinc finger and promyelocytic leukemia in leukemogenesis and development. *Curr Opin Hematol* 2001; **8**: 212–217.
- Barna M, Hawe N, Niswander L, Pandolfi PP. Plzf regulates limb and axial skeletal patterning. *Nat Genet* 2000; **25**: 166–172.
- Costoya JA, Hobbs RM, Barna M, Cattoretto G, Manova K, Sukhwani M et al. Essential role of Plzf in maintenance of spermatogonial stem cells. *Nat Genet* 2004; **36**: 653–659.

- 43 Seda O, Liska F, Krenová D, Kazdová L, Sedová L, Zima T *et al*. Differential linkage of triglyceride and glucose levels on rat chromosome 4 in two segregating rat populations. *Folia Biol (Praha)* 2003; **49**: 223–226.
- 44 Wieczorek D, Koster B, Gillessen-Kaesbach G. Absence of thumbs, A/hypoplasia of radius, hypoplasia of ulnae, retarded bone age, short stature, microcephaly, hypoplastic genitalia, and mental retardation. *Am J Med Genet* 2002; **108**: 209–213.
- 45 Fischer S, Kohlhase J, Böhm D, Schweiger B, Hoffmann D, Heitmann M *et al*. Biallelic loss of function of the promyelocytic leukaemia zinc finger (PLZF) gene causes severe skeletal defects and genital hypoplasia. *J Med Genet* 2008; **45**: 731–737.



This work is licensed under the Creative Commons Attribution-NonCommercial-No Derivative Works 3.0 Unported License. To view a copy of this license, visit <http://creativecommons.org/licenses/by-nc-nd/3.0/>

Supplementary Information accompanies the paper on the Nutrition and Diabetes website (<http://www.nature.com/nutd>)